CLOSED-LOOP SYSTEM IDENTIFICATION EXPERIENCE FOR FLIGHT CONTROL LAW AND FLYING QUALITIES EVALUATION OF A HIGH PERFORMANCE FIGHTER AIRCRAFT

Patrick C. Murphy
NASA Langley Research Center
Hampton, Virginia 23681-2199

SUMMARY

This paper highlights some of the results and issues associated with estimating models to evaluate control law design methods and design criteria for advanced high performance aircraft. Experimental fighter aircraft such as the NASA High Alpha Research Vehicle (HARV) have the capability to maneuver at very high angles of attack where nonlinear aerodynamics often predominate. HARV is an experimental F/A-18, configured with thrust vectoring and conformal actuated nose strakes. Identifying closed-loop models for this type of aircraft can be made difficult by nonlinearities and high-order characteristics of the system. In this paper only lateral-directional axes are considered since the lateral-directional control law was specifically designed to produce classical airplane responses normally expected with low-order, rigid-body systems. Evaluation of the control design methodology was made using low-order equivalent systems determined from flight and simulation. This allowed comparison of the closed-loop rigid-body dynamics achieved in flight with that designed in simulation. In flight, the On Board Excitation System was used to apply optimal inputs to lateral stick and pedals at five angles of attack: 5, 20, 30, 45, and 60 degrees. Data analysis and closed-loop model identification were done using frequency domain maximum likelihood. The structure of the identified models was a linear state-space model reflecting classical 4th-order airplane dynamics. Input time delays associated with the high-order controller and aircraft system were accounted for in data preprocessing. A comparison of flight estimated models with small perturbation linear design models highlighted nonlinearities in the system and indicated that the estimated closed-loop rigid-body dynamics were sensitive to input amplitudes at 20 and 30 degrees angle of attack.

NOMENCLATURE

b	number of eigenvector elements specified
C_{lp}	nondimensional aerodynamic rolling moment coefficient due to roll rate
$C_{n\beta}$	nondimensional aerodynamic yawing moment coefficient due to sideslip
d	number of measurements
m	number of controls
n	number of states
n_z	normal acceleration, g's
n_y	lateral acceleration, g's
p_{max}	maximum roll rate, deg/sec
p_s	stability-axis roll rate, rad/sec
r_s	stability-axis yaw rate, rad/sec
α	angle of attack, rad.
β	sideslip, rad.
ϕ	bank angle, rad
λ	eigenvalue
η_{ped}	pilot pedal input, lbs./105.38
η_{stick}	pilot lateral stick input, in./3.57
ω	frequency, rad/sec
ζ	damping ratio
τ_a	lateral stick input time delay
τ_r	rudder pedal input time delay
A/B	afterburner
ANSER	Actuated Nose-Strakes for Enhanced Rolling
AOA	Angle of Attack
CHR	Cooper-Harper flying qualities rating
CRAFT	Control Power Robustness Agility and Flying Qualities Tradeoffs
DEA	Direct Eigenspace Assignment
DR	Dutch Roll
HARV	High Alpha Research Vehicle
HATP	High Alpha Technology Project
HIL	Hardware-in-the-loop
MDA	McDonnell Douglas Aerospace
Mil-Std	Military Standard Specifications
MIMO	multi-input/multi-output
NL	nonlinear
OBES	On-Board Excitation System
PIO	pilot induced oscillation
PsC	Psuedo Controls
RMS	root mean square
S	Strake mode of ANSER control law
SID	System Identification
STV	Strake and Thrust-vectoring mode of ANSER control law
TV	Thrust-vectoring mode of ANSER control law

INTRODUCTION

An important step in flight control law development is a rigorous flight test program to test system performance, stability and control. As part of the flight test evaluations test pilots are typically required to assess the quality of manual control during specified maneuvers usually in terms of the Cooper-Harper rating scale [1]. Obtaining favorable pilot ratings may lead a designer to believe that the control design methodology was effective. However, without models identified from flight test data, representing the closed-loop dynamics of the system, there is only qualitative evidence that the design method was successful. Using system identification techniques to identify closed-loop models provides direct evidence as to whether the intended dynamics were achieved and can explain the cause of unexpected pilot ratings or aircraft behavior. To be completely successful, however, an important part of the identification process must also address the high-order and typically nonlinear characteristics of modern high performance aircraft systems.

This paper will provide some results of the closed-loop modeling effort performed during the NASA High-Alpha Technology Program (HATP) [2]. One goal of this program was to develop advanced control law design

methodologies for fighter aircraft with high levels of agility and high angle-of-attack (high-α) capability. This effort has provided the Actuated Nose Strakes for Enhanced Rolling (ANSER) control law [3]. The ANSER control law was designed for the NASA High Alpha Research Vehicle (HARV) and was flight tested over a three year period from 1994 to 1996. HARV is a highly modified F/A-18, configured with two novel control effectors: thrust vectoring and conformal actuated nose strakes. More details of these control effectors can be found in [4,5]. The lateral-directional control law was designed to use yaw thrust vectoring and forebody strakes individually or in combination. The longitudinal control law [6] uses pitch thrust vectoring throughout the flight envelope.

Control design methods and control design criteria were integral parts of the overall control design approach studied in the HATP program. The design methods used were a combination of CRAFT (Control Power, Robustness, Agility, and Flying Qualities Tradeoffs) [7] and Pseudo Controls (PsC) [8,9]. The combination of CRAFT and PsC is a hybrid design technique that combines both linear and nonlinear design methods. The design criteria used to develop the ANSER control law were taken from several sources covering a spectrum of design guidelines from those flight-validated and commonly used at low-α to high-α guidelines that are currently a subject of research. The goal of this hybrid technique was to develop a control law that would provide the HARV with agile maneuvering capability and Level 1 flying qualities in high-α flight. In addition, a complete set of nonlinear design guidelines [10] was used to design the final ANSER control law. Although the nonlinear design guidelines are an important aspect of the research in HATP, only linear flying qualities specifications are considered in this paper.

One goal of the system identification effort in HATP was to evaluate control design methods and control design guidelines for their success in developing the ANSER lateral-directional control law. To perform evaluations of both design method and design criteria, low-order equivalent systems (LOES) were estimated from both flight data and from nonlinear simulation data for comparison. These models are identified in the form of 4th-order state-space representations of the closed-loop system. Estimated state-space models were required for the control law evaluation since the control law design method directly defined the eigenspace for the low order, multi-input/multi-output (MIMO), closed-loop system. This approach allows comparison of low-order desired dynamics determined in the control law design process using CRAFT with low-order dynamics achieved in nonlinear simulation and in flight. Merit of the design methodology was determined by the degree of success in achieving the desired closed-loop dynamics. Flying qualities criteria was assessed by comparison of achieved dynamics with pilot ratings obtained in flight. This paper presents some of the system identification problems and issues that arose during the evaluation of the design methods and flying qualities design guidelines. The evaluation is restricted to the lateral-directional ANSER control law in thrust-vector (TV) mode without nose strakes activated.

CONTROL LAW OVERVIEW

A key set of objectives for the lateral-directional control law was to provide good flying qualities, robustness, and agility appropriate for an advanced fighter aircraft while respecting the control power limitations of the experimental vehicle. This included optimal blending of control effectors and management of system changes as the novel control effectors, thrust-vectoring and forebody strakes, are included in the control mix or as the conventional aerodynamic controls become ineffective at high α.

In the ANSER control system, lateral stick commands stability axis roll rate and pedals command a conventional body yaw rate response. The control law is designed for "feet on the floor" control by the pilot for normal coordinated flight. The feedback gains and pilot input gains were designed at twelve flight conditions (α: 5 to 60 degrees for every 5 degrees, $n_z=1g$, altitude=25K feet). Feedback gains were designed using the CRAFT method. In the control law the pilot input gains are scheduled with α, n_z, and altitude; and the feedback gains are scheduled with α. The measurements used for inner-loop feedback control are body axis roll rate, body axis yaw rate, lateral acceleration, and an estimated sideslip rate. The controls are aileron, rudder, differential stabilator, yaw thrust vectoring and actuated forebody strakes. Differential leading and trailing edge flaps were not used.

CRAFT and PsC were integrated to synthesize the lateral-directional control law for HARV. The Pseudo Controls method was applied to HARV as a way of allocating pilot commands to all the lateral-directional controls. For the HARV, an envelope was defined over a wide range of angle of attack, Mach number, and engine thrust settings. Pseudo Controls allows feedback design for a reduced problem, since it maps multiple control inputs into a minimum orthogonal set of control inputs. This maximizes the coordinated use of the available control power. In addition, the control law is simplified by substantially reducing the number of feedback gains. With this reduced system, CRAFT was used efficiently to determine the "optimum" eigenspace for a measurement feedback control law.

The CRAFT design approach determines linear, multivariable feedback gains by using Direct Eigenspace Assignment (DEA) [11] and a graphical framework to trade-off multiple and often conflicting design requirements. DEA provides a mechanism to determine measurement feedback control gains that produce an achievable eigenspace for the closed-loop system. It has been shown [12] that for a system that is observable and controllable with n states, m controls, and d measurements, one can exactly place d eigenvalues and m elements of their associated eigenvectors in the closed-loop system. DEA provides feedback gains that place b elements (m<b<n) of d eigenvectors associated with d eigenvalues through a least squares fit of the desired eigenvectors to the achievable eigenspace. The CRAFT method satisfies a need to incorporate multiple design requirements into the flight control design process. Design requirements that can be quantified are readily included. Generally, these requirements fall into one of four categories of design metrics: 1) control power, 2) robustness, 3) agility, and 4) flying qualities. Details of the CRAFT design process are presented in [7].

In the design process for HARV, due to the frequency separation between the rigid-body and higher-order modes the feedback design was performed on 4th order rigid-body lateral-directional models only. However, stability

analysis (gain and phase margin calculations) was done using full 26th order linear system model of the plant and control law. The 26th order model included actuator models, sensor models, compensation filters, aeroelastic models and corresponding notch filters. Nonlinear simulation allowed designers to uncover any limitations inherent in the linear analysis and allowed tuning of critical elements such as command gains. This portion of the development was followed by extensive piloted simulation and hardware-in-the-loop tests.

The flying qualities design criteria used to develop the ANSER lateral-directional control law are drawn from several sources. For low α, the commonly used Mil-STD 1797A [13] and the fighter-specific study of Moorhouse-Moran [14] were used. Moorhouse-Moran criteria was used as the preferred criteria. These criteria are shown in figures 1 and 2. The Cooper-Harper level 1 and level 2 regions of the Mil-Std criteria represent the largest areas and the Moorhouse-Moran the smallest areas. The desirable regions used in the Moorhouse-Moran study are much smaller than the Mil-Std because of the restricted nature of the tasks considered; these tasks were specifically tailored to modern high-performance fighter missions.

At the beginning of the control design effort, NASA sponsored McDonnell Douglas Aerospace (MDA) to develop flying qualities criteria at three stall and post-stall angles of attack. This work did not define Dutch Roll mode criteria, therefore the Moorhouse-Moran criteria was used except when control power limitations at $\alpha = 60$ degrees prevented the criteria from being met. The early MDA work was done concurrently with the HARV control law development and was reported in [15] and [16]. Lateral criteria were developed for stability-axis roll rate command systems. Figure 3 show flying qualities specifications [15] for desirable roll mode dynamics at high α for a lateral-directional fine-tracking maneuver. These criteria, presented in both low-order equivalent system modal parameter and bode envelope formats, have been refined and are summarized in reference [17].

CONTROL LAW DESIGN METHOD EVALUATION

For this report, the method evaluation will primarily focus on a comparison of desired versus achieved closed-loop rigid-body eigenvalues. This is a very focused view considering the wide variety of linear and nonlinear design guidelines affecting any control system design. For evaluation of the CRAFT-PsC design method, however, using the achieved linear dynamics as a primary evaluation metric is appropriate since an important result of the CRAFT design process is the determination of the best linear rigid-body dynamics for the aircraft. One design goal for the ANSER control law was to provide desirable rigid-body dynamics in fine-tracking maneuvers over a large range of α. Fine-tracking maneuvers require relatively small pilot inputs and therefore tends to produce linear responses, which supports using linear analysis of both flight and simulation results. Fine-tracking maneuvers, used in the HARV experiment, were designed to allow development of high-α flying qualities criteria and associated evaluation tasks. This work was done in simulation by McDonnell Douglas Corporation under task order contract to NASA LaRC and detailed task descriptions can be found in reference [17].

Linear Design Rigid-Body Dynamics

Rigid-body dynamics were defined over the entire range of α in conjunction with analysis of HARV capabilities, mission requirements, linear guidelines, and nonlinear guidelines that were also part of HATP research. The results of this analysis produced the HARV ANSER design goals for the rigid-body dynamics. These dynamics are shown in figure 4 as solid lines. Only the roll mode and Dutch Roll mode frquency and damping ratio are shown. Although the spiral mode was also included in the ANSER control law design, it is not a dominant mode and will not be shown in this paper. Dutch Roll mode specifications for low α, defined by Mil-Std 1797A level 1 requirements and Moorhouse-Moran, were assumed to be valid for high α. Mil-Std 1797A requires the product of Dutch Roll frequency and damping ratio to be greater than 0.4. As shown in figure 4, design goals of $\zeta_{DR}=0.7$ and $\omega_{DR} \geq 1.0$ are indicated over the entire range of α for HARV. MDA criteria, developed in simulation, were used as a guide for roll mode dynamics at α equal to 30, 45, and 60 degrees.

For the ANSER control law, the CRAFT design process used 4th-order linear plant models extracted from nonlinear simulation using a small perturbation approach to obtain the Jacobian matrices. Small perturbation models may be used for design purposes if the full nonlinear system has relatively mild nonlinearities and the linear models adequately describe the nonlinear system responses to small inputs. As the degree of nonlinearity increases, the small perturbation models can produce dramatically different models with only small changes in the trim operating point or in the size of perturbation. For the HARV simulation used in design, some substantial nonlinearities exist in the aerodynamic model, especially for α between 20 and 30 degrees. These nonlinearities found in wind tunnel studies have been flight validated by Klein [18].

The feedback gains used in the ANSER control law applied to the 4th-order design models of HARV in TV mode produce the dynamics indicated in figure 4 as the "low order linear" case. The differences between the design goals and the low order case are completely due to intentional changes in feedback gains to accommodate the S (nose strakes only) and STV (strakes and TV) modes. Although CRAFT provides a design tool that allows matching of design specifications, in this case, it does not lend itself to matching 3 distinct aircraft configurations, simultaneously, with one set of feedback gains. The movement of the rigid-body dynamics with the introduction of higher order dynamics is shown in figure 4 as the difference between the "low order" and "high order" cases. The results of increasing order of the system were a slight increase the speed of the Roll subsidence mode and Dutch Roll mode frequency as well as a small increase in Dutch Roll damping.

Rigid-Body Dynamics Achieved in Flight And Nonlinear Simulation

Low-order equivalent systems of the MIMO closed-loop system for ANSER-HARV in TV mode were estimated from flight data to provide a direct comparison with the corresponding design models estimated from simulated data. Both flight data and simulated data were sampled at

80 Hz. Corrections for sensor offsets from the center of gravity were applied to angle of attack, sideslip angle and accelerometer signals from flight. Angle of attack was corrected for upwash and small data compatibility corrections were also applied to the flight data.

Optimal inputs were designed for this study as a series of square waves optimized to maximize information content for a fixed time period [19]. The inputs are documented in references [20-22]. This method was chosen because only very short maneuver times were available. This constraint resulted from the limited time the test aircraft could remain at a given flight condition when testing at high α. Although modest changes in altitude did not dramatically change the system dynamics, the test aircraft had very large sink rates at high α and thus could significantly change the test condition if long test times were allowed. The input optimization technique also limited output amplitudes to avoid large deviation from the test condition. Test inputs were executed at the pilot station by a computerized On-Board Excitation System (OBES) after the pilot trimmed the aircraft at the specified test condition.

The estimated closed-loop models were linear, 4th order, lateral-directional models in state-space form. System states, $x = [\beta \ p_s \ r_s \ \phi]$, were sideslip angle, stability axis roll rate, stability axis yaw rate and bank angle. OBES inputs, $u = [\eta_{ped}(t-\tau_r) \ \eta_{stick}(t-\tau_a)]$, were rudder pedal force and lateral stick deflection normalized by factors of 105.38 and 3.57, respectively. Equivalent time delay parameters τ_r and τ_a were estimated to be 0.042 sec. and 0.038 sec., respectively, for the $\alpha=45°$ case. These values are representative over the α range studied. Equivalent time delay parameters were estimated separately in the time domain using the approach recommended in reference [13]. Final values for these parameters were formed by averaging response delays found for individual surfaces to the commanded input. Time delay parameters were applied to the inputs in the frequency domain before estimation and held fixed during estimation of the state-space systems to avoid parameter correlation problems. System outputs, $y = [\beta \ p_s \ r_s \ \phi \ n_y]$, were the four states and lateral acceleration. This form of the model allowed determination of the system eigenspace and thus direct comparison of design eigenvalues and eigenvectors achieved in nonlinear simulation versus the corresponding flight-achieved values. The closed-loop system eigenspace was the primary metric for verification of the CRAFT design methodology. The system matricies can be written as

$$A = \begin{bmatrix} Y_\beta & Y_{p_s} & Y_{r_s}-1 & \dfrac{g\cos(\theta_o)}{V_o}+Y_\phi \\ L_\beta & L_{p_s} & L_{r_s} & L_\phi \\ N_\beta & N_{p_s} & N_{r_s} & N_\phi \\ 0 & \dfrac{\cos(\gamma_o)}{\cos(\theta_o)} & \dfrac{\sin(\gamma_o)}{\cos(\theta_o)} & 0 \end{bmatrix} \quad (1)$$

$$B = \begin{bmatrix} Y_{\eta_r} & Y_{\eta_a} \\ L_{\eta_r} & L_{\eta_a} \\ N_{\eta_r} & N_{\eta_a} \\ 0 & 0 \end{bmatrix} \quad (2)$$

$$C = \begin{bmatrix} 1 & 0 & 0 & 0 \\ 0 & 1 & 0 & 0 \\ 0 & 0 & 1 & 0 \\ 0 & 0 & 0 & 1 \\ \dfrac{V_0}{g}Y_\beta & \dfrac{V_0}{g}Y_{p_s} & \dfrac{V_0}{g}Y_{r_s} & \dfrac{V_0}{g}Y_\phi \end{bmatrix} \quad (3)$$

$$D = \begin{bmatrix} 0 & 0 \\ 0 & 0 \\ 0 & 0 \\ 0 & 0 \\ \dfrac{V_0}{g}Y_{\eta_r} & \dfrac{V_0}{g}Y_{\eta_a} \end{bmatrix} \quad (4)$$

These system equations are very similar to the open-loop system equations except for parameters L_ϕ, N_ϕ, and Y_ϕ. These parameters account for a small feedback gain applied to bank angle by the control system. The controller provided gravity compensation during large bank angle rolls or multiple rolls by the aircraft.

Estimation of the closed-loop models was accomplished using a maximum likelihood method in the frequency domain after the model structure was determined using stepwise regression [23]. The frequency domain approach improved two steps in the identification process: (1) simplifies application of input time delays, and (2) automatically adjusts parameter error bounds to reflect the possibility of colored noise on the measurements [24].

Assuming a state-space model of the system, without process noise, the system can be written in the time-domain as

$$\dot{x} = Ax + Bu, \qquad x(0) = 0 \quad (5)$$
$$y = Cx + Du$$
$$z_i = y_i + v_i$$

where z_i is the discrete ith measurement of the output vector y and v_i is the ith measurement noise vector that is assumed to be from a zero mean Gaussian random process.

In the frequency domain, the system given by equation (5) can be written as

$$\tilde{x} = [i\omega I - A]^{-1} B\tilde{u}$$
$$\tilde{y} = C[i\omega I - A]^{-1} B\tilde{u} + D\tilde{u}$$
$$= G\tilde{u}$$
$$\tilde{z}_n = G_n\tilde{u}_n + \tilde{v}_n \quad (6)$$

where G represents the system transfer function matrix in the frequency domain. The measurement noise statistics can be written as

$$E(\tilde{v}_n) = 0; \qquad E(\tilde{v}_n\tilde{v}_n^*) = S_{vv} \quad (7)$$

where S_{vv} represents the spectral density of the measurement noise. The cost function, J, minimized to estimate the maximum likelihood parameters is

$$J = \frac{1}{2}[z_n - G_n u_n]^* S_{vv}^{-1}[z_n - G_n u_n] \quad (8)$$

where parameter estimates are obtained by minimizing $J(\theta)$ with respect to unknow parameters, θ. Because of the resulting nonlinear estimation problem a modified Newton-Raphson technique was used to find the minimum of $J(\theta)$. This approach is described in references [25] and [19].

System Identification maneuvers were performed at $\alpha = [5\ 20\ 30\ 45\ 60]$ degrees. Parameter estimates at $\alpha=45°$ are shown in the following table

Parameter Estimates for System at $\alpha=45°$

parameters	estimate	error bound
Y_β	-0.0600	0.0045
Y_{p_s}	0.0091	0.0017
$Y_{r_s}-1$	-0.9881	0.0030
Y_ϕ	-0.0053	0.0013
Y_{η_r}	-0.0072	0.0004
Y_{η_a}	-0.0104	0.0004
L_β	-3.1214	0.1213
L_{p_s}	-0.6685	0.0462
L_{r_s}	0.8559	0.1167
L_ϕ	-0.2467	0.0338
L_{η_r}	-0.1447	0.0177
L_{η_a}	0.0967	0.0118
N_β	2.7912	0.0506
N_{p_s}	0	*
N_{r_s}	-1.8258	0.0462
N_ϕ	0.2157	0.0222
N_{η_r}	0.4594	0.0107
N_{η_a}	0.2516	0.0078

* parameter excluded during model structure determination

Errors for the flight identified system matrix elements were typically 5% to 10% of their mean values and all parameters had error bounds less than 15%, except for Y_{p_s} and Y_ϕ. The relatively small values of these terms likely made accurate identification difficult and small values of $\phi(t)$ also made the Y_ϕ term less identifiable. Very large bank angles were avoided to maintain linear responses to inputs. Figures 5 and 6 show time histories for the flight data and estimated model at 45 degrees angle of attack. To produce time history comparisons a second estimation is required to obtain bias parameters. A time-domain maximum likelihood estimation was performed with the estimated model parameters held fixed at the values shown while bias parameters were allowed to vary.

Figure 7 shows the rigid-body dynamics from flight estimated models. The poles show a classical airplane distribution as was intended by design. For comparison with flight estimated values, the corresponding dynamics estimated from nonlinear simulation are presented in figure 7. The parameters in nonlinear simulation models were estimated in exactly the same manner as the flight models. For the simulation problem, the actual optimal inputs used in flight were applied to nonlinear simulation and the time histories were then treated as simulated flight data.

Reasonably good agreement between flight and simulation is shown in figure 7. The poles from simulation and flight follow the same trends as a function of α although some small differences occurred at certain points, such as, at α equal to 30 and 60 degrees for Dutch Roll frequency and 5 and 20 degrees for Dutch Roll damping. The roll mode shows good agreement. Nonlinear simulation was performed without measurement noise in order to determine the best case design results and to establish a benchmark for comparison with flight results.

One and two sigma error bounds for the flight-estimated pole locations are shown in figure 8 as light and dark shades around the pole mean values. Error bounds were obtained by using Monte Carlo simulation in which each estimated parameter of the system was allowed to vary with a uniform probability distribution over a range defined by the corresponding error bound for that parameter. The Monte Carlo simulation was run 5000 times to ensure coverage of all possible combinations and the eigenspace was determined for each new system to produce the plots in figure 8. One and two sigma boundaries provide a 68% and 95% confidence levels that the true value is contained within the indicated bounds. For $\alpha > 5$ degrees the two sigma bounds allow a range of roll and spiral poles that produces a complex mode with roll-spiral coupling. For the high-α range relatively small error bounds were obtained. In general, these results indicate reasonably accurate system identification.

In a formal evaluation of CRAFT, assessment of the complete system eigenspace achieved in flight would be required. However, for brevity, this paper will present rigid-body pole locations as the primary evaluation metric of both CRAFT and the high-α design criteria. Eigenvectors estimated from flight data matched those in simulation with accuracy comparable to that found for the eigenvalues. As an example, figure 9 shows eigenvectors achieved in flight compared with those achieved in nonlinear simulation at $\alpha = 30$ degrees. Eigenvectors are shown as bar graphs, where the dominant eigenvector element is used to normalize the eigenvector. The element magnitudes are plotted for models estimated from flight and from nonlinear simulation. The four bars represent the four eigenvector elements corresponding to the four states $[\beta$ (rad) p_S (rad/sec) r_S (rad/sec) ϕ (rad)]. The eigenvector comparison shows that the design modal shaping (from simulation) was achieved in flight reasonably well and that the shapes have a desirable aircraft form as intended.

System Identification Models vs Small Perturbation Models

Part of the design process for the ANSER lateral-directional control law required high-order linear models representing design points over the entire HARV flight envelope; these models were the primary tool for assessing stability margins. Creation of these models was accomplished by combining 4th-order, linear plant models with a linear model of the control law. In this form, a 26th-order linear perturbation model was obtained.

Figure 10 compares the rigid-body dynamics from high-order linear models with rigid-body dynamics from low-order equivalent systems obtained through system identification (SID) of flight and nonlinear simulation data. The low-order models identified from flight and

simulation are not obtained from small perturbations. They show the effects of system nonlinearities, such as rate limiting, that are not present in the small perturbation models. In addition, other nonlinearities, such as aerodynamic nonlinearities, will be expressed differently between the SID and small perturbation models. For both SID models and small perturbation models the nonlinearities create input-amplitude dependent variations in the models. However, because the amplitudes considered are quite different between the two approaches the resultant models can also be dramatically different. Careful assessment of nonlinearities is critical for any linear analysis of nonlinear systems.

Figure 10 shows reasonably good agreement between the SID models identified from flight and from nonlinear simulation. However, fairly large disagreement occurred between the SID models and the small perturbation models at $\alpha = 20$ and $\alpha = 30$ degrees. Since input amplitudes are orders of magnitude different between the two methods, nonlinearity must be investigated. Identifying SID models from simulation using a range of input amplitudes, allowed determination of a threshold input amplitude below which the estimated models' dynamics stopped changing. Figure 10 shows the poles from SID models where the input amplitudes were set at this threshold; the poles are identified as "low Amp NL Sim". These results were obtained by reducing the input amplitudes by 50% at $\alpha = 20$ degrees and by 40% at $\alpha = 30$ degrees. At $\alpha = 30$ degrees, the new SID model matches the small perturbation model. At $\alpha = 20$ degrees, further reduction of the input amplitude did not produce a significantly different model. The difference shown between these two cases at $\alpha = 20$ degrees is not resolved by adjusting SID input amplitude.

System Nonlinearities At $\alpha = 20$ Degrees

Two sources of error due to nonlinearity appear to exist since only a portion of the mismatch between SID and small amplitude models is explained by reducing input amplitude for the SID models. Another source of nonlinearity must explain the remaining mismatch at $\alpha = 20$ degrees. The difference between the reduced amplitude SID model and the small perturbation model at $\alpha = 20$ may be explained by considering the underlying plant aerodynamic model. Figure 11 shows $C_{l\beta}$ and $C_{n\beta}$ as a function of α. This data was taken from Klein [18] where wind tunnel data for the HARV was flight validated by comparison with flight estimated aerodynamic parameters. These two aerodynamic parameters are strongly responsible for defining the roll mode and Dutch Roll mode frequency, respectively. At $\alpha = 20$ degrees, $C_{n\beta}$ exhibits a dramatic nonlinearity directly affecting the Dutch Roll frequency and at slightly under $\alpha = 22$ degrees, $C_{l\beta}$ also exhibits a sharp nonlinearity affecting the roll mode. The variation of α during the flight experiment was approximately ±4 degrees from trim for all test points greater than $\alpha = 5$ degrees. This ensures that the nonlinearities at $\alpha = 20$ degrees were experienced during flight. Unless a flight experiment is designed specifically to capture a nonlinearity this sharp and the small perturbation model is developed respecting this characteristic, it is very difficult to achieve a match between SID and small perturbation models. Additional

unknown nonlinearities may have been introduced since β perturbations were slightly larger than expected during the flight experiment.

A second source of nonlinearity is predominantly due to rate limiting of the control surfaces. Rate limiting can produce a strong nonlinearity in the response data. In the simulation of the ANSER HARV system the no-load rate limit of the rudders is 82 deg/sec and under the loads experienced maneuvering at $\alpha = 20$ degrees, the loaded rate limit was approximately 75 deg/sec. For the same α maneuver in flight, the rudders rate limited at approximately 72 deg/sec for the right rudder and 67 deg/sec for the left rudder. To assess the effects of rate limiting, a metric defining the percent of time the surfaces experienced rate limiting was defined. The percent-of-time metric is computed as the percent of time during maneuver that the surface rate exceeds a specific threshold appropriate for that surface. The threshold for rudders, ailerons, and vanes was set at 60 deg/sec. The threshold for stabilators, which have substantially slower actuators, was set at 30 deg/sec. These thresholds reflect the loaded rate-limit capability of the stabilators and rudders, in particular.

Figure 12 shows the percent of time the surfaces experienced rate limiting for each α case considered. As shown in the figure, both rudder surfaces spent more than 35% of maneuver time in rate limit for the $\alpha = 20$ degrees case and more than 27% of maneuver time in rate limit for the $\alpha = 30$ degree case. By reducing the input amplitudes to the low amplitude thresholds, discussed previously, the percent time metrics were reduced to 18% and 9% for the cases where α was 20 and 30 degrees, respectively. It appears that a modest amount of rate limiting can be tolerated in flight and still allow reasonable dynamic matching of linear models between small perturbation models and SID models from flight. With rate limit metric values in the range of 10-15% the small perturbation models and SID models from flight have a reasonable match.

An Experiment Design Issue

A concern in designing the experiment for identification of closed-loop models from flight was finding input amplitudes that would strike a balance between being small enough to keep the responses in the linear range but large enough to keep response levels adequate for SID. Early in the flight test program, test pilots were asked to apply optimal inputs manually to the stick and pedals. OBES was not available during this testing. Although manual inputs have been used successfully in other flight test experiments, the spectrum and sequencing of the inputs are limited. These early flight tests were done using optimal inputs with lateral stick input amplitudes of approximately 1.5 inches and full pedal input amplitudes of 100 lbs. These tests were repeated using the same input form but with half the amplitude. The results indicated that half amplitude manual inputs were insufficient to produce adequate response information for SID. Unfortunately, the half amplitude inputs were representative of the amplitudes used by the pilots in fine-tracking maneuvers. In light of these results, more aggressive, full-amplitude inputs were designed for use with OBES to ensure good signal to noise ratios and adequate system excitation for SID. These inputs

were intentionally designed to maximize the response of the system and even allow a small amount of rate limiting.

The results in figure 10 and 12 indicate that the inputs for the test points at α equal to 20 and 30 degrees were too aggressive. Two factors contributed to this result. First, the control law command gains were large in this region in order to satisfy agility requirements. Second, the rate limits of the rudder actuators in flight were slower than expected. Limited test time prevented further testing to determine if OBES inputs could be reduced to provide adequate data with smaller input amplitudes. Fortunately, the match between simulation and flight models is reasonably good when comparable inputs are used to estimate models. This gives some confidence that the SID models determined with the lower amplitudes from simulation may represent the correct dynamics for the system. In addition, the match between simulation and flight time histories during fine-tracking is very good. In light of this, the dynamics experienced by HARV pilots during fine-tracking maneuvers is best represented in figure 10 by the flight and simulation models for all α except at α =[20 30] degrees. For these two cases, the best available representation of system dynamics is more likely given by "low Amp NL Sim" model dynamics.

System Dynamics: Variation With Normal Acceleration

An issue that arises when evaluating the high-α flying qualities design criteria is whether the SID models estimated from 1g flight correctly predict the dynamics corresponding to that occurring during fine tracking of a turning target aircraft. Although pilots are using relatively small inputs during fine tracking and therefore should be in the linear response range, fine tracking does occur in a loaded condition. Time histories for fine tracking maneuvers at α = 30 degrees show the flight loads are approximately 2 g's. For fine tracking at α equal to 45 and 60 degrees, the flight loads fall to approximately 1.5, g's. To address this question, the closed-loop rigid-body dynamics from models trimmed at 1 and 2 g's are presented in figure 13. This comparison is made using the low-order, closed-loop, linear design models (small perturbation models) for 1 and 2 g's. The results indicate that the roll mode is only slightly affected by g load over most of the α range. There is an increase in roll mode eigenvalue for α = 5 degrees and a modest decrease in value for α = 60 degrees. The Dutch Roll mode, on the other hand, is generally affected uniformly over the entire α range considered. Dutch Roll mode frequency is increased with an increased g load and Dutch Roll damping ratio is decreased.

The high-α design criteria provides roll mode specifications only at α equal to 30, 45, and 60 degrees [17]. The roll mode dynamics given in figure 10 were determined from 1g flight data and 1g simulation data using SID techniques at 5 α's. These roll mode dynamics can be compared with the high-α design criteria and should correctly represent that experienced in flight during fine tracking maneuvers. However, at α = 30 degrees, the most plausible estimate for roll mode during fine tracking is given by the low amplitude simulation value. Comparison of 1g model dynamics with the design criteria can be done for the following reasons: (1) the roll mode is not substantially changed under a 2g load for a range of α

extending from 10-50 degrees; and (2) although figure 13 indicates some reduction in roll mode eigenvalue at α = 60 degrees with a 2g load, the fine tracking maneuvers of interest at this α reach only 1.5 g's.

Dynamics Achieved in Flight vs Design Dynamics: Flying Qualities Summary

Achieving good flying qualities during fine-tracking maneuvers was an important design goal for the ANSER lateral-directional control law. To help judge the success of the control law, figures 14 and 15 display closed-loop rigid-body poles for ANSER (TV mode) in relation to the flying qualities criteria. The variation of these dynamics with α is also shown. The poles displayed are from three sources: (1) design goals; (2) flight-achieved dynamics; and (3) rate-limited dynamics.

Design goals (1) are the intended dynamics defined by high-order linear perturbation models. Flight-achieved dynamics (2) represent the rigid-body dynamics estimated from flight data, except at α equal to 20 and 30 degrees where excessive rate limiting occurred during the SID maneuvers. At these two α's, the best estimates of the flight-achieved dynamics, when rate-limiting is not occurring, is given by the "low Amp NL Sim" models. These models are estimated using nonlinear simulation responses to flight SID inputs with reduced amplitudes. This provides the best estimate of the dynamics experienced by pilots during fine tracking maneuvers in lieu of actual low input-amplitude flight data. During fine tracking maneuvers pilots are using sufficiently small inputs that actuator rate limiting is minimized and linear responses are obtained. Rate-limited dynamics (3), at α equal to 20 and 30 degrees, define the dynamics obtained with relatively large inputs. These are estimated from fight data where full-amplitude SID maneuvers resulted in excessive actuator rate limiting.

Figure 14 provides the Dutch Roll criteria from Mil-Std 1797A and the Moorhouse-Moran study. The boundaries indicated are for Level 1 flying qualities during Class IV, Category A flight at low α. For this study it was assumed to be valid over the entire α range. Superimposed on this graphic are the Dutch Roll poles for the 5 flight test points from α = 5 to 60 degrees. The plot shows that all the criteria were satisfied except for the flight-achieved Dutch Roll damping ratio at α = 60 degrees. At this flight condition the damping ratio fell below the design goal of 0.4 to 0.31. This was likely caused by a lack of control power since at this α the stabilator is position limited (differential stabilator provides some yaw control) and thrust-vectoring pitch priority logic is used.

Figure 15 provides the roll mode criteria from Moorhouse-Moran for low α and from MDA for α = 30 degrees. Roll pole locations representing the flight-achieved dynamics are plotted on this chart as roll mode time constants for each of the 5 test points. The corresponding design goals are also shown for these five points as well as two additional values at α equal to 10 and 35 degrees. All the low-α (≤10°) roll poles are well within the Moorhouse-Moran design criteria. The high-α roll poles from α = 20 to 35 degrees, although somewhat low relative to the criteria, still satisfy the requirements. Although no criteria

is provided for α equal to 45 and 60 degrees, the design values and achieved values are shown for comparison. Both design and flight-achieved poles are plotted with very low roll rate sensitivity values reflecting the low control power (relative to the criteria) available to the HARV vehicle at high α. Also shown is the substantial effect of rate-limiting on roll mode characteristics at α equal to 20 and 30 degrees. At both α's the roll mode time constant was approximately doubled in response to the rudders rate limiting more than 25% of the maneuver time. This moved the poles well out of the desirable regions for α equal to 20 and 30 degrees and into the α = 60 degrees region.

SID Issues Presented by Stick Characteristics

The MDA criteria uses stability axis roll rate sensitivity as a means of capturing both the roll rate capability and stick characteristics in one metric. Stick characteristics play an important roll in the pilot's perception of aircraft flying qualities, and since relatively small commands are used for fine-tracking maneuvers, roll rate sensitivity is a more appropriate metric than, for example, maximum roll capability. In the HARV-ANSER control system a nonlinear stick shaper is used to optimize the pilot's handling qualities. The shaper is a smooth parabolic function which allows full command authority by rapidly increasing stick sensitivity for relatively large input commands and reduces stick sensitivity for relatively small commands.

The stick shaper is not a dynamic element in the control law; it does, however, modify the pilot's commands. Because of these characteristics the stick shaper is a double-edged sword for the SID problem. The nonlinear shaper makes designing excitation inputs more difficult by modifying inputs, however, since it is not a dynamic element it does not change estimated system eigenvalues. A key concern for both the control law designer and the SID input designer is that the command inputs are not large enough to produce nonlinear responses such as rate-limiting. This type of nonlinear response will dramatically change the dynamics of the closed-loop system, as shown in figure 15.

Since the estimated eigenvalues are independent of the nonlinear stick shaper an assumption of 1 inch stick inputs is made to determine roll rate sensitivity and make all the plots with respect to the MDA flying qualities criteria. This value represents the size of maximum inputs normally required by pilots to perform fine-tracking maneuvers. This assumption is also supported by the shaper being approximately linear for small inputs.

CONTROL LAW DESIGN CRITERIA EVALUATION

High-α design criteria were developed in fixed-base piloted simulation with a variety of tracking tasks reflecting the gross acquisition and fine tracking. Control power and actuator limitations were not addressed in that study. In order to properly compare the flight estimated models and pilot ratings of this flight experiment with the design criteria it is necessary to use the "low Amp NL Sim" models for the 20° and 30° α cases. This should provide the best estimate of system dynamics experienced by the pilots. Although the "low Amp NL Sim" models are estimated from the nonlinear simulation, these models match flight time histories. In addition, the simulation and flight-estimated

model dynamics also matched well under rate-limited conditions.

Pilot ratings were determined using a Cooper-Harper scale [1] for tasks specifically designed to address the fighter fine-tracking task. This task, although well defined, still allows pilot's discretion as to the piloting method to achieve the goals of fine tracking. Consequently, it is possible to have different input characteristics for the same task. To demonstrate this, the statistics of three pilot's inputs were computed by estimating the mean, standard deviation, and maximum input over each pilot's flights. As shown in figure 16, a sample of three pilots performing the same fine tracking task at 30° α, indicates quite different input statistics. The figure shows a bar chart of the pilot's mean input (absolute value) during fine tracking. Pilots are indicated by the research program's pilot labels of D, E, and A, respectively. The mean values are small as would be expected for a fine tracking maneuver where the pilot frequently returns to a steady position on a smoothly turning target. The standard deviation bar chart characterizes the amplitude of each pilot's stick motion. Pilot E has substantially larger stick inputs during these maneuvers. The bandwidth of these inputs (not shown) was also dramatically higher compared with pilots D and A. The maximum deflection chart highlights the magnitude of the inputs for each pilot. Pilot E chose an approach for tracking with almost full command and at very high frequency. This would be more in line with a gross acquisition task or a task requiring very rapid maneuvering. Discussions with pilot E indicated a strong interest in detecting sensitivity to PIO. The result of large amplitude inputs, as was shown for the aggressive SID models, is severe rate limiting in the rudders. Consequently, substantially different dynamics were experienced by pilot E. In light of this result, pilot E's ratings must be associated with the rate-limited dynamics and not with the design values.

Figure 17 shows the linear design criteria for both low and high α, the best estimates of the roll mode dynamics experienced by pilots D, E, and A during fine-tracking, and the corresponding pilot's Cooper-Harper ratings. For the α = 30 degrees case where pilot E used large enough inputs to experience significant rudder rate-limiting the pole location is indicated with a * and the corresponding CHR is shown. No pilot ratings were obtained at low α. However, the low-α roll mode dynamics are indicated to show their relative position to the high-α results. For cases where rate limiting was not an issue, the pilot ratings shown in brackets represent an average rating from each pilot. Pilots D and A are shown at 30 α, pilots D, E, and A are shown at 45 α, and pilots D and E are shown at α = 60 degrees. One of the pilots flew the maneuvers at least three times for the cases with α equal to 30 and 45 degrees. The pilot rating for the rate-limited dynamics at α = 30 degrees was obtained from a single run using pilot E.

It appears that the dynamics achieved in flight resulted in a system that is mostly near the lower boundaries of the MDA criteria. At α = 30 degrees, the average pilot rating of CHR=3 agrees with the MDA level 1 boundary. The rate-limited pole location obtained in flight at α = 30 degrees suggests a level 2-3 boundary. CHR's of 3 and 4 by pilots D and A using low amplitude inputs, at α = 45 degrees,

suggests this may be near a level 1-2 boundary. At $\alpha = 45$ degrees, pilot E's CHR of 7 for the lateral-directional axis may have reflected deteriorated dynamics in the longitudinal axis which was rated by pilot E as CHR=8. Pilot E's large amplitude inputs caused rate limiting in the longitudinal axis causing poor dynamic response and may have caused cross contamination of the ratings. At $\alpha = 60$ degrees, a CHR=7 by two pilots clearly suggests the dynamics were undesirable, however, the Dutch Roll damping ratio was not within level 1 requirements and may have caused the poor ratings. This pole location may define a boundary between level 2 and level 3.

CONCLUDING REMARKS

Estimating linear, closed-loop, low-order equivalent systems facilitated evaluation of both the control law design method and the high angle-of-attack flying qualities design criteria. However, the results highlight several issues that should be considered before adopting this approach. Strong agreement existed between dynamics identified from flight and simulation at all α. However, at α equal to 20, 30 and 60 degrees the flight achieved dynamics were not as closely matched to the design goals determined by small perturbation models from simulation. At $\alpha = 20$ degrees, this was most likely due to a combination of rate limiting and very nonlinear plant aerodynamics. Errors due to rate limiting were removed from the simulation results by reducing input amplitudes. The remaining difference between the small perturbation model and the estimated model using system identification is believed to be related to the nature of small pertrubation models. Errors in small perturbation models can be magnified depending on the size of small perturbations selected to obtain Jacobian matrices from nonlinear systems. At $\alpha = 30$ degrees the difference between flight and simulation estimated models with the small perturbation model was completely accounted for by reducing input amplitude and correspondingly reducing the amount of rate limiting. A likely cause of mismatch at $\alpha = 60$ degrees may be lower levels of control power in flight than predicted by the small perturbation model. The small perturbation models in this study highlighted the nonlinear effects from rate limiting and from the basic aircraft aerodynamic model, particularly at α equal to 20 and 30 degrees.

These results highlight the fact that for flight test experiments of high performance aircraft several issues need to be considered in the experiment design. One issue concerns the degree of nonlinearity of the system under study. Careful experiment design, flight test, and data analysis are required but some a priori knowledge of the system may be required to account for certain system nonlinearities, especially strong nonlinearities that are not well modeled by classical rigid-body airplane models. Planning for linear, LOES identification experiments should include multiple input amplitudes to provide a basis for testing the degree of nonlinearity. Identifying the limits of validity the LOES is also needed when nonlinear responses are possible. Finding the limits of estimated linear models is similar in importance to estimating error bounds for the model parameter estimates. Separate analysis and identification of the control law and aerodynamic model might be required to determine the sources of some errors or nonlinearities. The same consideration should be applied to less classical higher

order systems, although that issue was not experienced with the lateral-directional system presented in this study due to the large frequency separation between the controller dynamics and the closed-loop, rigid-body dynamics. For this study, it was shown that these potential error sources can be overcome and accurate models can be identified from flight test if certain measures are taken to compensate for the various sources of error. Parameter error bounds of up to 10% on the estimated model parameters were estimated. The highest error bounds were associated with parameters which are typically very small and do not contribute significantly to the response.

An observation from this study is the importance of checking the validity of small perturbation models taken from full nonlinear simulatons. These models are typically used in control design and analysis to model the open-loop and closed-loop plant characteristics. Whether used in design or analysis a series of perturbation amplitudes for generating these models should be used to test the sensitivity of the plant dynamics to perturbation size. Linear models obtained from small perturbations can produce dynamics significantly in error depending on the degree of nonlinearity of the basic aerodynamic model. A check of the linear model responses against nonlinear simulation or the flight vehicle responses should be made at expected nominal operating input and response amplitudes. If nonlinearities exist, system identification methods may be preferred over small perturbation techniques to obtain linear design models. This would allow estimation of linear models that represent the nonlinear system as it operates with nominal input and response amplitudes. However, some strong nonlinearities may preclude the use of LOES altogether.

The percent of time actuators spend in rate limit was used effectively to highlight the nonlinear effect on linear dynamics. Although this was an effective metric for this study, it is not clear that the rate limit metric could be universally applied to any maneuver. The maneuvers used in this study were of the same duration and the optimal inputs had similar power spectrums designed to excite rigid-body dynamics. Comparing maneuvers with dramatically different input types may lead to errors in the comparison of percent time in rate limit. However, it may be useful to determine the appropriate benchmark value for each case or use the percent time metric with a specific input design specifically to test for such nonlinearity.

Another issue related to experiment design is to account for the sometimes different piloting techniques used by test pilots. In this study, the variation of input amplitude and frequency spectrum among the pilots produced dramatically different flying qualities evaluations. For modern high performance fighters the potential for amplitude dependent nonlinear response is very high and should be anticipated during the experiment design. For flying qualities evaluations, identification of models characterizing the system that pilots experience while performing fine tracking maneuvers needs consideration.

REFERENCES

1. Cooper, George E., and Harper, Robert P., Jr.: The Use of Pilot Rating in the Evaluation of Aircraft Handling Qualities. NASA TND-5153. April 1969.

2. Foster, J.V.; Bundick, W. T.; Pahle, J.W.: Controls for Agility Research in the NASA High-Alpha

Technology Program. SAE TP-912148. September, 1991.

3. HARV Control Law Design Team, "Design Specification for a Thrust-Vectoring, Actuated-Nose-Strake Flight Control Law for the High-Alpha Research Vehicle", NASA Technical Memorandum 110217.

4. Murri, D. G., Shah, G. H., DiCarlo, D. J., and Trilling, T. W., "Actuated Forebody Strake Controls for the F-18 High-Alpha Research Vehicle", Journal of Aircraft, Vol. 32, May-June, 1995.

5. Bundick, W. T., Pahle, J. W., Yeager, J. C., Beissner, Jr., F. L., Design of a Mixer for the Thrust-Vectoring System on the High-Alpha Research Vehicle. NASA TM 110228. June 1996.

6. Ostroff, A. J., Proffitt, M. S., "Longitudinal-Control Design Approach for High-Angle-of-Attack Aircraft", NASA TP 3302. February 1993.

7. Murphy, P.C., Davidson, J.B., Control Design for Future Agile Fighters. Presented at AIAA Atmospheric Flight Mechanics Conference. AIAA Paper No. 91-2882. August 1991.

8. Lallman, F. J., Relative Control Effectiveness Technique With Application to Airplane Control Coordination, NASA TP 2416, April, 1985.

9. Lallman, Frederick J.: Preliminary Design Study of a Lateral-Directional Control System Using Thrust Vectoring. NASA TM-86425, November 1985.

10. Hoffler, K.D.; Brown, P.W.; Phillips, M.R.; Rivers, R.A.; Davidson, J.B.; Lallman, F.J.; Murphy, P.C.; and Ostroff, A.J.: Evaluation Maneuver and Guideline Development For High-Alpha Control Law Design Using Piloted Simulation. AIAA Paper No. 94-3512. August, 1994.

11. Davidson, J. B., Schmidt, D.K., Flight Control Synthesis for Flexible Aircraft Using Eigenspace Assignment. NASA CR-178164. June 1986.

12. Srinathkumar, S.: Modal Control Theory and Application to Aircraft Lateral Handling Qualities Design, NASA TP-1234, June 1978.

13. Mil Std 1797A, Military Standard - Flying Qualities of Piloted Aircraft, January, 1990.

14. Moorhouse, D.J.; Moran, W. A.: Flying Qualities Design Criteria For Highly Augmented Systems. IEEE National Aerospace and Electronics Conference, NAECON May 20-24, 1985.

15 Kreckler, G.C., Wilson, D.J., Riley, D.R., High Angle-of-Attack Flying Qualities Criteria. AIAA 28th Aerospace Sciences Meeting, AIAA 90-0219, Jan. 8-11, 1990.

16. Wilson, D.J., Riley, D.R., Flying Qualities Criteria Development Through Manned Simulation for 45° Angle of Attack-Final Report. Vol. 1 and 2. NASA CR 4435. April 1992.

17. Wilson, D. J. and Citurs, K. D., "High Angle-of-Attack Flying Qualities Design Guidelines," NASA

Contractor Report 4681, Volumes I and II, February, 1996.

18. Klein,V., Ratvasky, T. R., Cobleigh, B. R., Aerodynamic Parameters of HARV Estimated From Flight Data. NASA TM 102692. August, 1990.

19. Morelli, E.A.: Optimal Input Design for Closed Loop Modeling at High Angles of Attack. AIAA paper 96-3418, AIAA Atmospheric Flight Mechanics Conference. San Diego, California. July 1996.

20. Morelli, E.A.: Piloted Parameter Identification Flight Test Maneuvers for Closed Loop Modeling of the F-18 High Alpha Research Vehicle (HARV). NASA CR 198268. February 1996.

21. Morelli, E.A.: Flight Test Maneuvers for Closed Loop Lateral-Directional Modeling of the F-18 High Alpha Research Vehicle (HARV) using Forebody Strakes. NASA CR 198270. February 1996.

22. Morelli, E.A.: Parameter Identification Flight Test Maneuvers for Closed Loop Modeling of the F-18 High Alpha Research Vehicle (HARV). NASA CR 198269. February 1996.

23. Klein,V., Batterson, J.G., and Murphy, P.C.: Determination of Airplane Model Structure From Flight Data by Using Modified Stepwise Regression", NASA TP-1916, 1981.

24. Morelli, E.A., and Klein, V.: Determining the Accuracy of Maximum Likelihood Parameter Estimates with Colored Residuals. NASA CR 194893. March 1994.

25. Klein, V. "Aircraft Parameter Estimation in Frequency Domain", AIAA paper 78-1344, Atmospheric Flight Mechanics Conference, Palo Alto, CA, August 1978.
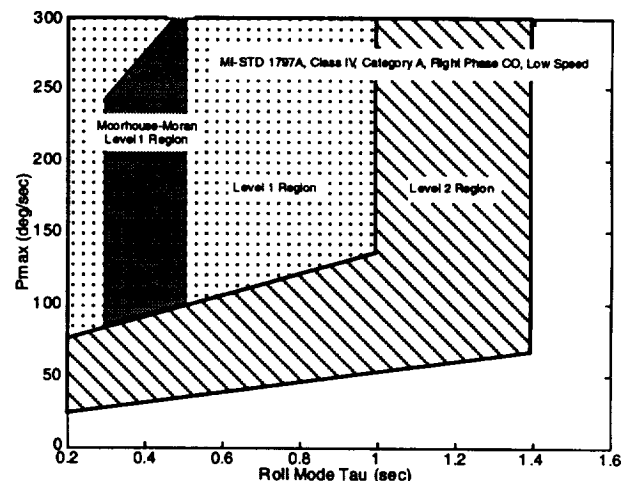
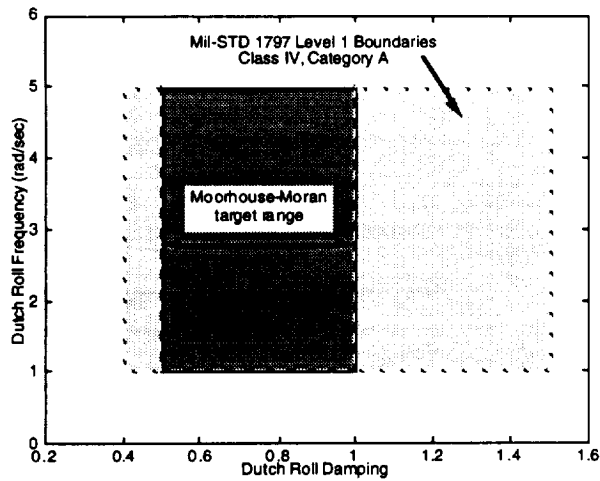Figure 1. Roll mode specifications for low AOA.

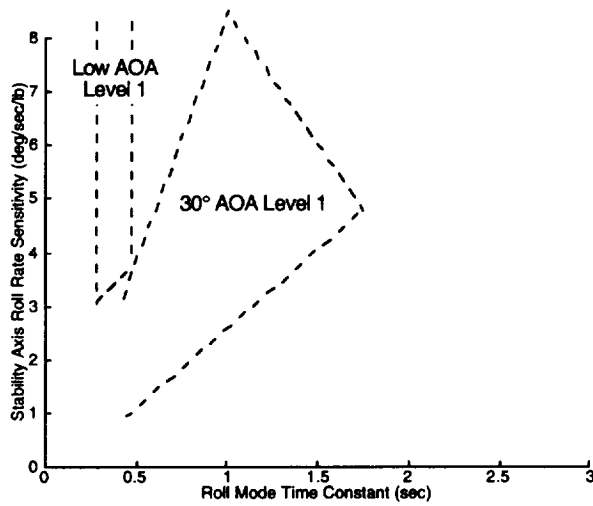Figure 2. Dutch Roll mode specifications for low AOA.

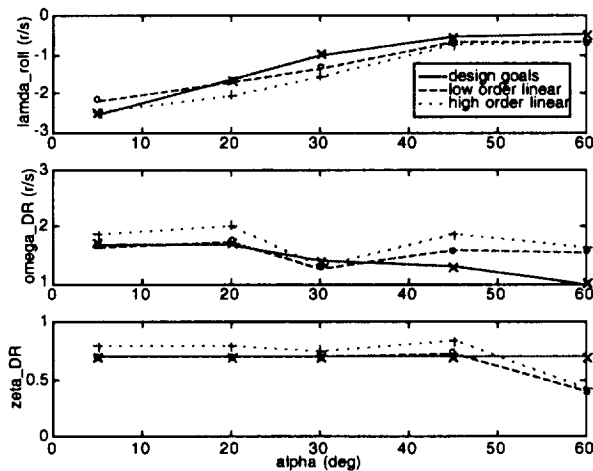Figure 3. Roll mode specifications for fine-tracking maneuvers.

Figure 4. Rigid-body poles for design, 4th and 26th order models in TV mode.
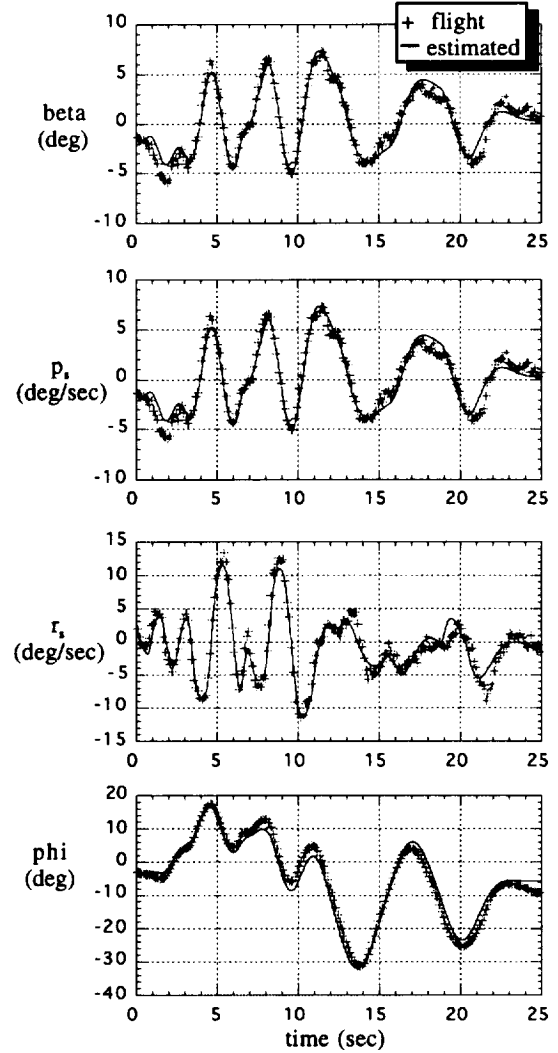

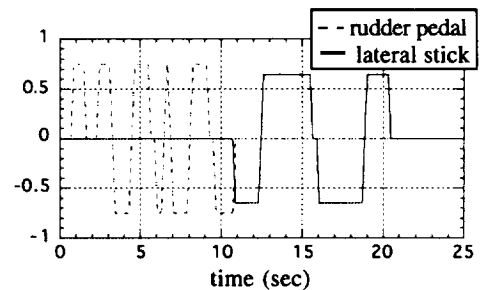Figure 5 Sample time histories of measured and estimated responses at 45 degrees angle of attack.

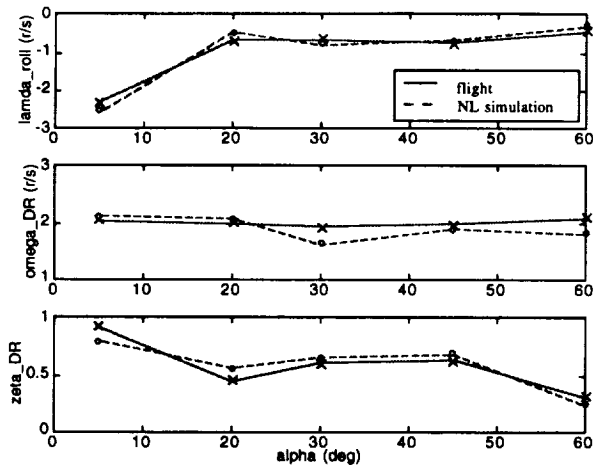Figure 6. Sample input time histories to rudder pedal and lateral stick at 45 degrees angle of attack.

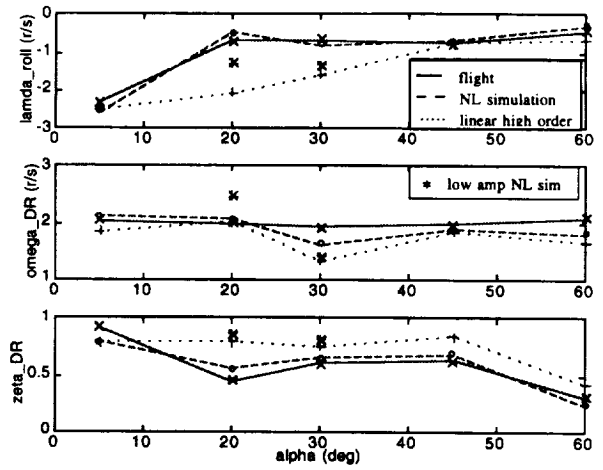Figure 7. Rigid-body poles from SID models obtained
using flight and simulation data.

Figure 10. Rigid-body dynamics determined with large and
small amplitude inputs.
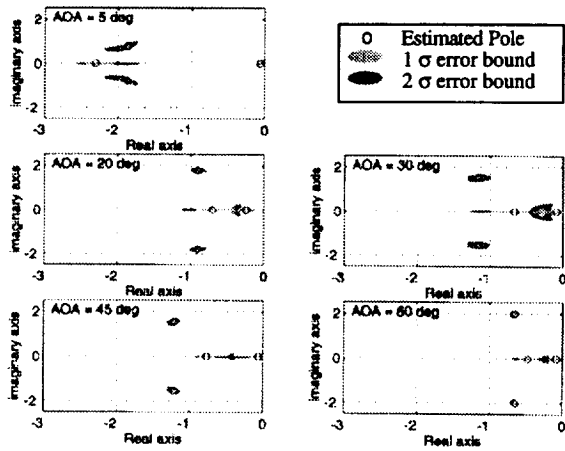
Figure 8. Flight estimated rigid-body poles with error
bounds.
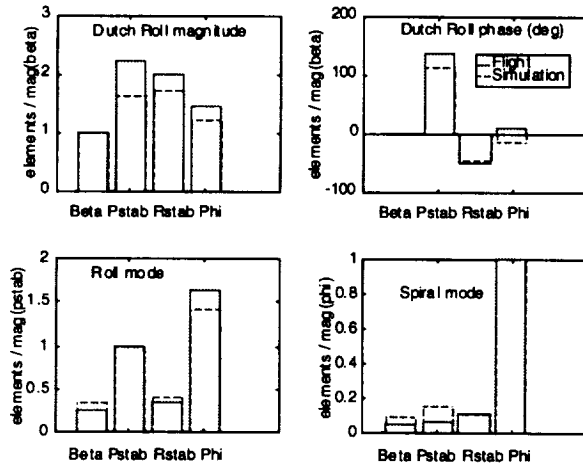
Figure 9. Stability axis eigenvectors estimated from flight
and simulation SID models at 30° AOA
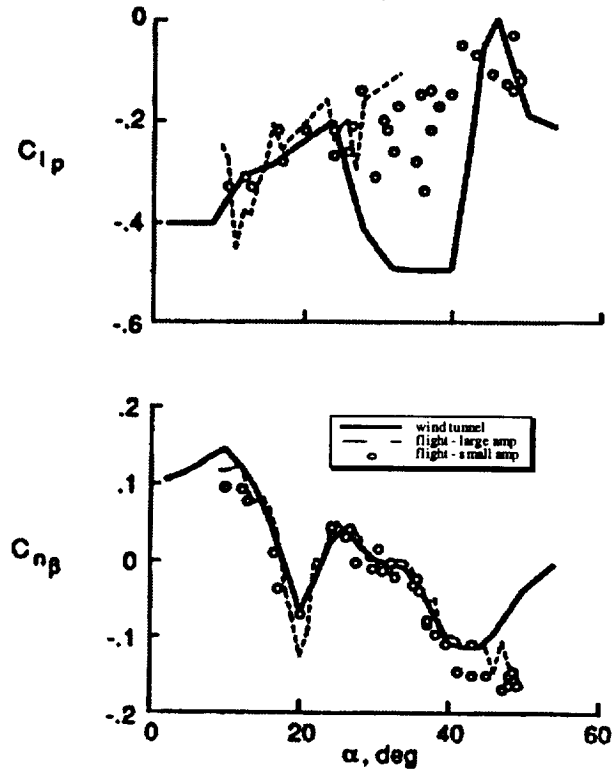
Figure 11. Aerodynamic parameters of HARV estimated
from flight and wind tunnel data.
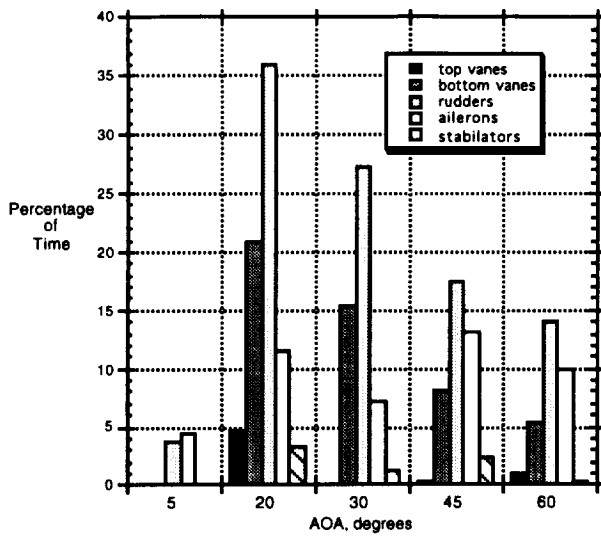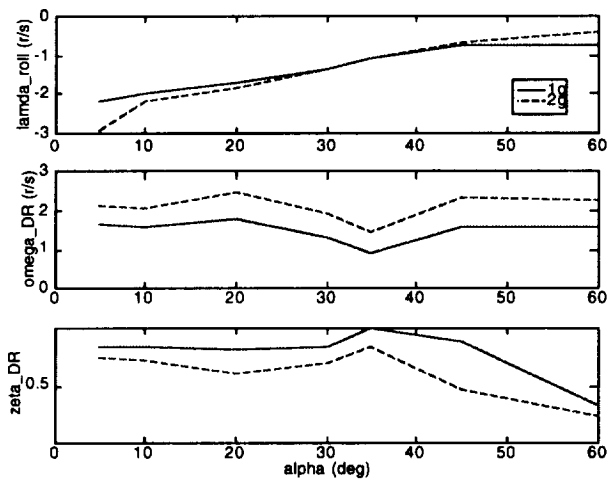
Figure 12. Percentage of time control surfaces were in rate limit during SID maneuvers.

Figure 13. Variation of closed-loop rigid-body dynamics with normal acceleration.
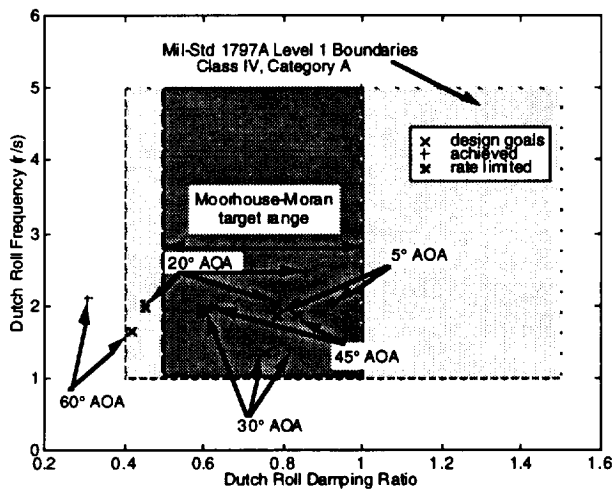
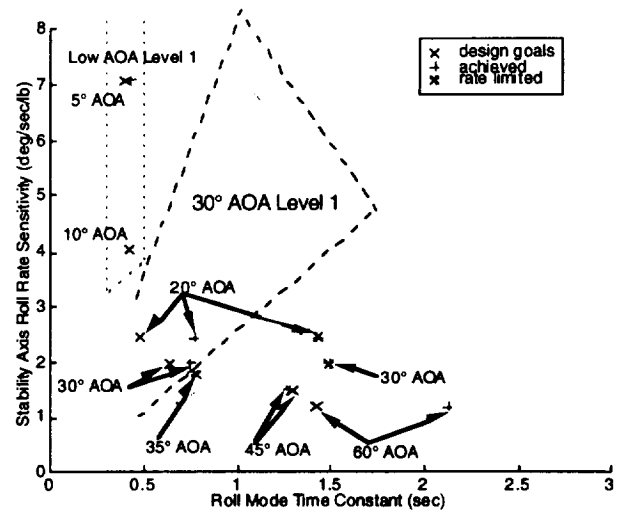Figure 14. Dutch Roll poles with respect to flying qualities criteria.

Figure 15. Roll mode poles with respect to flying qualities criteria.
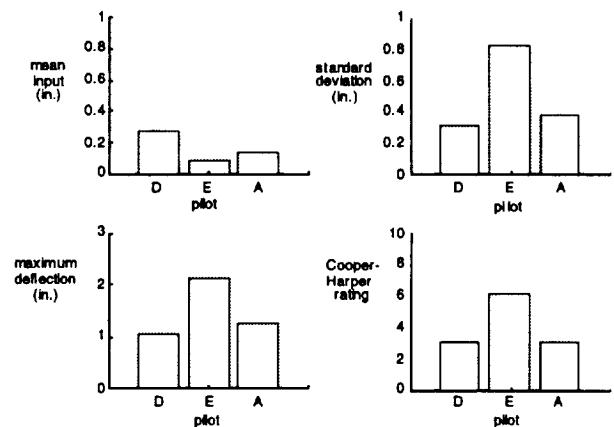

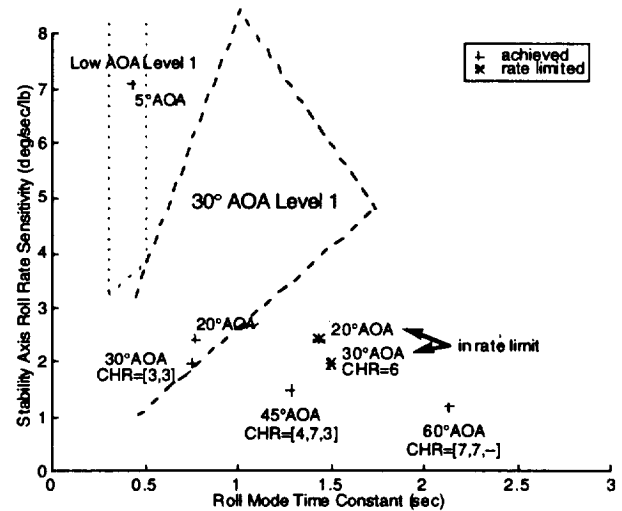Figure 16. Pilot input characteristics during fine-tracking maneuvers at 30° AOA.

Figure 17. Pilot ratings for fine-tracking maneuvers vs flying qualities criteria.